

REVIEW ARTICLE

Targeted delivery of anti-cancer growth inhibitory peptides derived from human α -fetoprotein: review of an International Multi-Center Collaborative Study

GJ Mizejewski¹, M Mirowski³, P Garnuszek², M Maurin², BD Cohen⁴, BJ Poiesz⁵, GA Posypanova^{6,7}, VA Makarov⁷, ES Severin⁸, and SE Severin^{6,7}

¹Wadsworth Center, New York State Department of Health, Empire State Plaza, Albany, New York, USA, ²Department of Radiopharmaceuticals, National Medicines Institute, Warsaw, Poland, ³Department of Pharmaceutical Biochemistry, Laboratory of Molecular Biology and Pharmacogenomics, Medical University, Lodz, Poland, ⁴Science and Engineering Center, Department of Biological Sciences, Union College, Schenectady, New York, USA, ⁵Regional Oncology Center, Division of Hematology/Oncology, SUNY Upstate Medical University, Syracuse, New York, USA, ⁶Moscow Research Institute of Medical Ecology, Moscow, Russia, ⁷Institute of Molecular Medicine of I.M. Sechenov Moscow Medical Academy, Moscow, Russia, and ⁸Russian Research Center for Molecular Diagnostics and Therapy, Moscow, Russia

Abstract

The α -fetoprotein derived growth inhibitory peptide (GIP) is a 34-amino acid peptide composed of three biologically active subfragments. GIP-34 and its three constituent segments have been synthesized, purified, and studied for biological activity. The GIP-34 and GIP-8 have been characterized as anticancer therapeutic peptides. A multicenter study was initiated to elucidate the means by which these peptide drugs could be targeted to tumor cells. The study first established which cancer types were specifically targeted by the GIP peptides in both *in vitro* and *in vivo* investigations. It was next demonstrated that radiolabeled peptide (¹²⁵I GIP-34) is specifically localized to rodent breast tumors at 24 h post-injection. The radionuclide studies also provided evidence for a proposed cell surface receptor; this was confirmed in a further study using fluorescent-labeled GIP-nanobeads which localized at the plasma membrane of MCF-7 breast cancer cells. Finally, it was readily demonstrated that GIP conjugated to either fluorescein or doxorubicin (DOX) underwent tumor cell uptake; subsequently, DOX-GIP conjugates induced cytotoxic cell destruction indicating the utility of GIP segments as cancer therapeutic agents. Following a discussion of the preceding results, a candidate cell surface receptor family was proposed which correlated with previous published reports for a putative AFP/GIP receptor.

Keywords: α -Fetoprotein; AFPep; cancer cells; cell surface; growth inhibitory peptide; P149 peptide; receptors; targeted delivery

Introduction

The growth inhibitory peptide (GIP) derived from human α -fetoprotein (HAFF) is a biologically active 34 amino acid peptide (GIP-34) composed of three subfragments designated as GIP-12 (P149a), GIP-14 (P149b), and GIP-8 (P149c, AFPep) (Mizejewski et al., 1996; Vakharia & Mizejewski, 2000; Mizejewski, 2007). The 34-mer

segment lies buried in a molecular cleft that is exposed as a result of stress/shock exposures such as oxidative shock (Mizejewski, 2001). While all three subfragments display bioactivity in a variety of *in vitro* and *in vivo* models, GIP-34 and GIP-8 (AFPep) have consistently demonstrated anticancer therapeutic activity in a multitude of published reports (Mizejewski & MacColl, 2003; Muehleemann et al., 2005; Torres, Pino, & Sierralta, 2009).

Address for Correspondence: GJ Mizejewski, Wadsworth Center, New York State Department of Health, Empire State Plaza, Albany, NY 12201, USA. E-mail: mizejew@wadsworth.org

(Received 19 November 2009; revised 16 December 2009; accepted 27 December 2009)

ISSN 1061-186X print/ISSN 1029-2330 online © 2010 Informa UK, Ltd.
DOI: 10.3109/10611861003587243

<http://www.informahealthcare.com/drt>

RIGHTS LINK
Copyright Clearance Center

The GIP-34 suppresses growth by S-phase cell cycle arrest and p27 inhibitor stabilization (Mizejewski et al., 2006a); while GIP-8 acts via blockage of serine-118 phosphorylation of the estrogen receptor at its N-terminal A/B trans-activation domain and by modulation of p21 inhibitor activity (Mesfin et al., 2001). Since GIP-8 constitutes part of the GIP-34 segment, the 34-mer peptide is capable of regulating both p27 and p21 cell cycle inhibitors. Overall, GIP-8 functions largely in estrogen (E)-dependent cell systems, while GIP-34 is active in both E-dependent and E-independent cell models (Mizejewski, 2007). The GIP-8 segment, discovered by one of the present authors (GJM), has also been referred to as AFPep in several recent publications (Mesfin et al., 2000; Bennett et al., 2002). Bennett, Mesfin, and others have since confirmed, extended, and scrutinized the use of GIP-8 as an anticancer agent (for a review, see Mizejewski, 2007).

All four GIP peptides (GIP-34, GIP-12, GIP-14, GIP-8) have been synthesized, purified, and characterized according to classical biochemical methodologies including high pressure liquid chromatography (HPLC), mass spectroscopy, amino acid (AA) composition, isoelectric point determination, AA sequencing, circular dichroism, and hydrophobicity/hydrophilicity plotting (MacColl et al., 2001). Secondary structure analysis revealed that GIP-34 was an amphipathic peptide consisting of 45% β -sheet, 45% random coil (disorder), and 10% α -helix. In addition, GIP-34 and GIP-8 have a single C-terminal Type-I reverse β -hairpin turn (Mesfin et al., 2001; Mizejewski & MacColl, 2003; Mizejewski, 2007). The reverse β -turn has been shown to enhance the biological activity of ligand binding because cell surface receptor topology is known to preferentially accommodate the β -turn conformation in ligand-to-receptor binding kinetics (Shields, 2009). The reverse β -turn is readily apparent in GIP-34, which has been demonstrated to bind to the surface of human breast cancer cells followed by rapid internalization into the cytoplasm (Mizejewski & MacColl, 2003). Preliminary findings have also reported the transmembrane passage of GIP-8 into cancer cells. It has been proposed that GIP-34 and GIP-8 (and full-length AFP) bind to an unknown cell surface receptor, undergo receptor-mediated endocytosis, and reside in the endosome vesicle system (Mizejewski, 2002).

Historical

It is evident from previous reports that GIP-34 can serve as a ligand which binds to a receptor(s) on tumor cell surfaces (Mizejewski & MacColl, 2003). Clearly, GIP-34 is also capable of suppressing tumor proliferation in both rodent and human cancer *in vitro* and *in vivo* models. It was further shown that GIP's biological activity is dependent on its oligomeric state, specifically its

linear compared with cyclic configuration (Muehleemann et al., 2005). In studies using cell adhesion assays, it was demonstrated that GIP-34 inhibited tumor cell attachment against various extracellular matrix (ECM) proteins, many of which serve as basement membrane and anchor constituents (Mizejewski & MacColl, 2003; Mizejewski et al., 2006). In assays using activated platelet suspensions and MCF-7 cells, GIP-34 was shown to be able to block all stages of platelet aggregation and tumor cell adhesion against various ECM proteins (Mizejewski et al., 2006; Mizejewski, 2007). Finally, the use of isolated membrane preparations possessing ACETYLcholinesterase as a reporter enzyme showed that GIP-34 enhanced cell membrane vesicle formation (Mizejewski et al., 2006; Mizejewski, 2007). Overall, the inhibition by GIP-34 of cell surface activities such as tumor cell adhesion, migration, and platelet aggregation was shown to seriously impair the ability of tumor cells to spread, adhere, and metastasize.

Although the initial step in the mechanism of GIP's tumor growth suppression has been proposed as cell membrane receptor blockade of G-protein-linked signaling cascades, the precise mode of cell membrane interaction and ligand uptake is yet to be elucidated (Muehleemann et al., 2005). Previous studies have also shown that the growth inhibitory property of GIP-34 is observed across species barriers and is seen in insects, amphibians, birds, and mammals including man and rodents (Butterstein & Mizejewski, 1999; Butterstein, Morrison, & Mizejewski, 2003; Mizejewski, Smith, & Butterstein, 2004). These observations suggest a growth inhibitory mechanism of action of GIP-34 that is common to different kinds of animal cell/tissues and indeed, S-phase cell cycle arrest was found to be the common cause (Mizejewski et al., 2006). This shared event accompanying GIP's inhibitory activity appears to be initiated as cell surface events following the attachment of GIP to plasma membrane receptors, which in turn, trigger cytoskeletal-mediated cell shape/form changes and endocytosis (Mizejewski, 2004). Such activities indicate that GIP-34 is a plasma membrane interactive agent that can interfere with cell membrane-induced signal transduction pathways which are involved in tumor growth, progression, and metastasis (Mizejewski et al., 2006).

Previous studies have documented that α -fetoprotein binds to an unknown but measurable AFP-receptor (AFP-R) with various binding affinities on different human tumor cells and lymphocytes (Uriel et al., 1984a; Villacampa et al., 1984; Torres, Geuskens, & Uriel, 1992b; Kanevsky et al., 1997). The AFP-binding proteins were detectable in membrane-bound forms exhibiting various molecular weights (Uriel et al., 1984a; Mizejewski, 1995). Mouse mammary tumors (*in vivo*) preferentially incorporated radiolabeled AFP when compared with normal tissue (Uriel et al., 1984b). Recent studies have shown

that AFP-R is clearly associated with both fetal and neoplastic tissues (Biddle & Sarcione, 1987; Lorenzo et al., 1996; Kanevsky et al., 1997). The expression of the AFP-R on human non-proliferating cells is very low; for example, the number of AFP-R molecules on lymphoma cells is about 10 times higher than on normally proliferating T lymphocytes (Torres et al., 1989). Such observations have provided the impetus for studies in which AFP has been used as a vector for anticancer drug delivery (Severin et al., 1995; Severin, 1996).

The present review has presented efforts to demonstrate that cancer cells express AFP-R molecules which can be utilized for *in vivo* biodistribution and *in vitro* binding studies of fluorescent and radiolabeled GIP. These studies demonstrate GIP's potential application for the diagnosis and therapy of cancerous tumors.

The EMTPVNPG (AFPep) octapeptide comprises the GIP-8 fragment, which contains amino acid residues 489–496 of the human AFP-derived GIP-34; this segment endows the GIP segment with the capability to suppress estrogen-dependent growth of the immature mouse uterus and breast tumors (Mizejewski, 2007). It was shown that this octapeptide and its linear and cyclic analogues (in which prolines are replaced with hydroxyprolines) inhibited the proliferation of estrogen-dependent breast tumor cells *in vitro* and *in vivo* (Mesfin et al., 2000, 2001; Bennett et al., 2002). It was further reported that the octapeptide was able to inhibit angiogenesis in chicken embryos and human tumors (Mizejewski et al., 2006) as well as tumor cell adhesion to the ECM (Mizejewski, 2007). It was also demonstrated, that both GIP-34 and GIP-8 reduced the fetotoxicity produced from both estrogens and insulin *in vivo* similar to intact AFP (Butterstein et al., 2003). In contrast to GIP-34, the octapeptide does not bind the intracellular estrogen receptor (ER α) or estradiol itself (Butterstein et al., 2003; Mizejewski, 2007).

Objectives

In the present multicenter collaborative report, several models of AFP-derived GIP targeting activities at the tumor cell membrane are presented in a review format. Following a historical review of the varied and multiple activities of GIP-34 and its subfragments (see earlier), a case was made to present the 34-mer peptide and its inclusive segments as cell surface interacting agents capable of influencing cell adhesion, shape, and form (Mizejewski et al., 2004; Muehleemann et al., 2005; Mizejewski, 2007). Second, several mammalian cell assays of *in vitro* and *in vivo* oncogenic growth are displayed in tabular form establishing and confirming GIP's growth suppressive capabilities in a myriad of human cancer cells and tissue types. The GIP growth inhibition was then compared with

small molecule drugs such as doxorubicin (DOX) and tamoxifen. Third, the tissue radio-distribution of labeled GIP-34 in mammary tumor-bearing rodents *in vivo* was presented concerning GIP-peptides labeled with either ^{125}I or $^{99\text{m}}\text{Tc}$. Following the biodistribution analysis, tumor tissue extracts were studied using cross-linking agents to isolate proteins binding to the labeled peptide. Fourth, the binding of GIP-34-coated fluorescent nanobeads to the surface of MCF-7 breast cancer cells was analyzed to determine binding specificity of GIP versus control peptides and to identify tumor binding proteins by cross-linking experiments. Finally, studies were conducted in which the cell uptake and retention of the GIP-8 fragment was analyzed by fluorescent microscopy utilizing ovarian tumor cells; these studies were followed by cell uptake studies employing DOX-conjugated 8-mer peptide. Overall, the present review has focused on the effects of GIP on cell surface events on neoplastic cells undergoing growth and progression with the aim of identifying GIP's molecular and cellular targets. Such studies should aid in elucidating the cell surface mechanism of action of GIP regarding early binding and uptake events (day 1) which ultimately result in tumor growth suppression by peptide treatment days 6 to 8.

Results

Growth effect of GIP-34 on human tumor cell lines

A summary of the screening of the GIP-34 peptide by the National Cancer Institute (NCI) Therapeutics Drug Screening Program (Bethesda, MD, USA) using many different human cancer cell lines has been reported. These findings detailed the *in vitro* results of GIP exposure to cell culture lines representing a variety of human cancer cell types (Mizejewski & MacColl, 2003; Muehleemann et al., 2005). In a 6-day proliferation assay (employing sulforhodamine staining), the linear GIP-34 peptide was reported to be cytostatic (non-cytotoxic) against 38 of the 60 NCI cancer cell lines, representing nine different cancer cell types including prostate, breast, and ovarian cancers and others (Muehleemann et al., 2005; Mizejewski et al., 2006). In subsequent reports, the effective use of the GIPs against various breast cancers has been reported in several studies involving breast cancer cells both *in vivo* and *in vitro* employing alternate day peptide doses over a 6–8 day testing period in cultures containing 5% fetal bovine sera (FBS) (Mizejewski, 2007). It was evident from those studies that both cyclic GIP-34 and linear GIP-8 were inhibitory against several breast cancers, including MCF-7 and T47D, as determined by sulforhodamine-stained cell proliferation assays. These studies indicated that both GIP segments have a growth inhibitory range from 40% to 90% at 10^{-7} M against a multiplicity of breast and prostate (reproductive) tumors.

Present *in vivo* experiments employing hollow fiber assays (Hollingshead et al., 1995) performed by the National Cancer Institute Therapeutics Group showed that GIP-34 achieved growth suppressions of 20–45% at day 4 showing its greatest effect against ovarian tumors (Table 1). These assays demonstrated that GIP-34 not only permeated the hollow fiber pores, but suppressed growth in tumor cells bathed within the body cavity of the host animal.

It was next deemed necessary to determine whether the various subsegments of GIP-34 exhibited tumor suppressive capabilities similar to those of the intact 34-mer peptide. The linear GIP was used because the subfragments did not form cyclic compounds for comparison. In studies employing a human kidney tumor cell line, it was further demonstrated that linear GIP-34 and its inclusive fragments (GIP-12, 14, 8) demonstrated different growth inhibitory capabilities. For example, GIP-34 displayed nearly 80% growth inhibition of kidney tumors at 5×10^{-4} M, while fragments GIP-14, GIP-12, and GIP-8 showed lesser potencies of 50%, 25%, and 20%, respectively (Mizejewski et al., 2006). As reported in previous cancer models, the individual subfragments of GIP-34 displayed less biological activity than the entire 34-mer peptide (Mizejewski & MacColl, 2003; Mizejewski et al., 2006; Mizejewski, 2007).

In a subsequent study using lymphomas, liver, and breast cell cultures in a 2 day versus a 7-day single dose study, it was determined that both linear and cyclic GIP-34 suppressed tumor growth from 20% to 84% that of controls (Table 2). It was evident that a single injection

of peptide in 10% FBS was highly suppressive at day 2; however, the single-dose effect did not endure for 7 days and appears to require alternate day doses as previously proposed (Mizejewski & MacColl, 2003). The peptides were most effective at 10^{-5} to 10^{-8} molar concentrations, and when compared to DOX and tamoxifen (40–100% suppressive), the peptides suppressive effect compared closely to tamoxifen, but was highly surpassed by the DOX inhibition. In some instances, GIP-34 exceeded the growth inhibition produced by both DOX and TAM, such as with MCF-7, BT-483, BT-549, and HUT-78. The GIP-34 peptides were most effective in the following tumor sequence: lymphomas > breast tumors > liver tumors. GIP showed little or no activity against normal lymphocytes, breast sarcomas, soft tissue and bone sarcomas, and tissue slices of bone osteoclast cells in culture (Table 2). In summary, it appeared that GIP-34 was effective against many epithelial cancers (adenocarcinomas) but not against tumors of sarcoma origin. In view of these experiments, one could propose that cyclic and linear GIPs should be either combined or conjugated with DOX and tamoxifen for *in vitro* studies, and this is demonstrated in the following text.

Biodistribution of radiolabeled GIP

A 34-amino acid-modified fragment of GIP-34 (designated as P149-QY), having two additional amino acids (glutamine and tyrosine), was synthesized and radiolabeled with ^{125}I radionuclide (Garnuszek et al., 2005). The introduction of a tyrosine residue at the C-terminal end

Table 1. Comparison of % growth/inhibition of the hollow fiber assay of linear GIP-34 versus 12 different tumors of six cell culture cancer types. Inhibition was observed at concentrations of 10^{-5} to 10^{-7} M. Hollow fiber (HF) *in vivo* results at day 4 are compared to the *in vitro* results at day 2 and day 6 of cell culture.**

S. No	Tumors used (Type and number code)	<i>In vitro</i> cell culture*	<i>In vivo</i> hollow fiber†	<i>In vitro</i> cell culture*
		2 days	4 days	6 days
1	Lung NCI-H23, H 226	5% (10^{-7})	†33% (10^{-6})	10% (10^{-7})
2	Lung NCI-H522, H460	30% (10^{-7})	33% (10^{-5})	80% (10^{-7})
3	Breast MDA-MB-231	25% (10^{-7})	16% (10^{-7})	70% (10^{-7})
4	Breast MDA-MB-435	20% (10^{-6})	30% (10^{-6})	80% (10^{-6})
5	Colon SW620, HCC-299	10% (10^{-6})	25% (10^{-6})	75% (10^{-6})
6	Colon 205	10% (10^{-7})	25% (10^{-6})	10% (10^{-5})
7	Melanoma LOX	20% (10^{-6})	24% (10^{-5})	50% (10^{-6})
8	Melanoma Uacc-62	20% (10^{-7})	8% (10^{-6})	80% (10^{-6})
9	Ovary Ovar-3	20% (10^{-7})	30% (10^{-6})	80% (10^{-7})
10	Ovary Ovar-4,5	20% (10^{-6})	42% (10^{-6})	85% (10^{-6})
11	CNS U251	15% (10^{-7})	26% (10^{-5})	45% (10^{-7})
12	CNS SF-295	25% (10^{-6})	20% (10^{-5})	80% (10^{-6})

GIP-34, linear 34-mer growth inhibitory peptide.

4 day HF, data obtained from hollow fibers (containing tumor cells) implanted into the body cavity of adult mice for a 4-day treatment with GIP-34.

*Cell culture assayed at day 2 and at day 6 using the Sulforhodamine stained procedure. Culture fluid contained 5% fetal bovine sera.

**Both the *in vitro* and the *in vivo* assays were performed by the National Cancer Institute Drug Screening Program (Bethesda, MD and Frederick, MD). The hollow fiber testing was conducted by Dr. Melinda Hollingshead (Frederick, MD) and the cell culture assays were performed under the direction of Dr. Anthony B. Mauger (Bethesda, MD).

†Hollow fiber assay of growth inhibition observed after intraperitoneal (I.P.) and subcutaneous (SC) injections of linear GIP-34.

Table 2. The growth suppressive effect (%) of CGIP-34 and LGIP-34 are shown at optimal concentrations for multiple types of tumor cells in culture using 10% fetal bovine serum. The peptide results are compared to treatment with doxorubicin and tamoxifen showing growth suppression at their optimal concentrations. All drugs and peptides were given at a single dose lasting for either 2 days or 7 days.

Tissue of origin	Cell line designation	Tumor or cell type	Growth suppression (%) and optimal conc. (M)				
			CGIP-34	LGIP-34	DOX	TAM	
*Lymph nodules	Hut-78	T-cell Lymphoma	2D	83 (10 ⁻⁷)	84 (10 ⁻⁵)	99 (10 ⁻⁵)	44 (10 ⁻⁶)
			7D	0 (-)	0 (-)	99 (10 ⁻⁶)	10 (10 ⁻⁶)
*Lymph nodules	Hut-102	T-Cell Lymphoma	2D	44 (10 ⁻⁷)	66 (10 ⁻⁷)	80 (10 ⁻⁶)	44 (10 ⁻⁶)
			7D	20 (10 ⁻⁷)	18 (10 ⁻⁷)	100 (10 ⁻⁶)	38 (10 ⁻⁵)
*Normal lymphocyte	None	PHA activated T-cell	2D	84 (10 ⁻⁸)	82 (10 ⁻⁶)	74 (10 ⁻⁵)	69 (10 ⁻⁵)
			7D	0 (-)	0 (-)	77 (10 ⁻⁵)	70 (10 ⁻⁵)
*Liver	HEPG2	Hepatoma	2D	46 (10 ⁻⁷)	80 (10 ⁻⁸)	90 (10 ⁻⁶)	60 (10 ⁻⁵)
			7D	0 (-)	0 (-)	100 (10 ⁻⁶)	60 (10 ⁻⁷)
*Breast	HCC1143	Breast Metastasis to the Liver	2D	50 (10 ⁻⁸)	Lys (10 ⁻⁵)	ND	ND
			7D	0 (-)	0 (-)	ND	ND
*Breast	T-47D	Ductal-carcinoma	2D	0 (-)	98 (10 ⁻⁸)	87 (10 ⁻⁶)	74 (10 ⁻⁵)
			7D	0 (-)	0 (-)	85 (10 ⁻⁶)	71 (10 ⁻⁷)
*Breast	BT 483	Ductal-carcinoma	2D	22 (10 ⁻⁸)	29 (10 ⁻⁶)	11 (10 ⁻⁶)	0 (-)
			7D	39 (10 ⁻⁵)	75 (10 ⁻⁷)	52 (10 ⁻⁶)	60 (10 ⁻⁶)
†Breast	MCF-7	Adeno-carcinoma	2D	88 (10 ⁻⁸)	48 (10 ⁻⁸)	72 (10 ⁻⁶)	63 (10 ⁻⁷)
			7D	0 (-)	0 (-)	91 (10 ⁻⁶)	70 (10 ⁻⁵)
*Breast	MDA-MB-157	Adeno-carcinoma	2D	0 (-)	5 (10 ⁻⁶)	6 (10 ⁻⁵)	0 (-)
			7D	36 (10 ⁻⁷)	35 (10 ⁻⁸)	100 (10 ⁻⁶)	87 (10 ⁻⁵)
*Breast	MDA-MB-468	Adeno-carcinoma	2D	21 (10 ⁻⁸)	23 (10 ⁻⁷)	33 (10 ⁻⁵)	0 (-)
			7D	38 (10 ⁻⁷)	17 (10 ⁻⁷)	100 (10 ⁻⁶)	100 (10 ⁻⁵)
*Breast	BT 549	Adeno-carcinoma	2D	50 (10 ⁻⁶)	50 (10 ⁻⁶)	10 (10 ⁻⁶)	0 (-)
			7D	6 (10 ⁻⁷)	6 (10 ⁻⁷)	100 (10 ⁻⁶)	48 (10 ⁻⁵)
*Breast	ZR75-1	Adeno-carcinoma	2D	0 (-)	0 (-)	ND	ND
			7D	50 (10 ⁻⁶)	50 (10 ⁻⁶)	98 (10 ⁻⁶)	69 (10 ⁻⁵)
†Breast	TX-2-28	Tamoxifen Resistant Adeno-carcinoma	2D	24 (10 ⁻⁷)	30 (10 ⁻⁶)	67 (10 ⁻⁶)	80 (10 ⁻⁷)
			7D	0 (-)	0 (-)	98 (10 ⁻⁶)	61 (10 ⁻⁵)
†Breast	MCF-10	Benign Adenoma	2D	0 (-)	0 (-)	0 (-)	0 (-)
			7D	12 (10 ⁻⁷)	48 (10 ⁻⁶)	100 (10 ⁻⁶)	97 (10 ⁻⁶)
§Soft Tissue	RD	Rhabdomyosarcoma	7D	0 (-)	0 (-)	ND	ND
§Bone	TC-71	Ewing's Sarcoma	7D	0 (-)	0 (-)	ND	ND
‡Bone	DORA-1	Osteoclasts	2D	ND	0 (-)	ND	ND

ND, not done; 2D, 2 days; 7D, 7 days; CGIP, cyclic growth with inhibitory peptide; LGIP, linear growth inhibitory peptide.

*Assayed by Bernard Poiecz, MD, Hematology/Oncology Department, University Hospital, Upstate Medical Center, Syracuse, New York.

†Assayed by Kathleen Arcaro, PhD, Department of Veterinary & Animal Sciences, University of Massachusetts, Amherst, Massachusetts. Data extracted from presentation at AACR Annual Meeting, Proc Amer Assoc Cancer Research, Washington, D.C., 2005.

‡Assayed by David Dempster, MD, Regional Bone Center, Clinical Pathology Department, Columbia University Medical Center, New York, NY (personal communication, unpublished data).

§Assayed by Timothy Damron, MD, Musculoskeletal Sciences Research Center, Department of Orthopedic Surgery, SUNY Upstate Medical Center, Syracuse, NY (personal communication, unpublished data.)

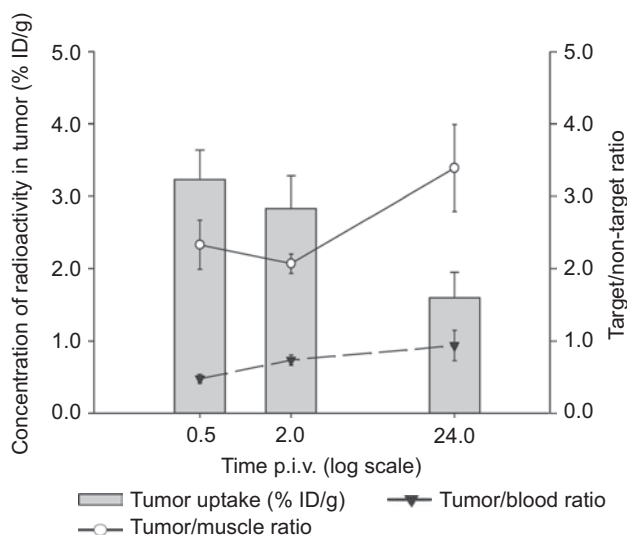
of GIP-34 enabled the preparation of the radioiodinated P149-Q^[125I]Y peptide. The P149-Q^[125I]Y was synthesized and then purified on a SPE C18 cartridge. The biodistribution studies employed the radioiodinated peptide injected into C3H/W mice bearing transplantable mammary adenocarcinomas. It was found that more than 40% and about 70% of the injected dose of P149-Q^[125I]Y were excreted into the urine at 2 h and 24 h post administration, respectively (Table 3) (Garnuszek et al., 2005). Relatively high accumulation in the stomach [18–20% of the injected dose per gram (ID/g)] was observed, suggesting either degradation or some unknown binding activity of the radioiodinated peptide *in vivo* (see

Discussion section). However, the constant amount of radioactivity retained in the stomach together with the decreasing concentrations of activity in the thyroid gland did not indicate a continuous release of free radioiodine (Table 3). Moderate and decreasing uptakes in the tumor tissue were also observed from 3.23% to 1.60% ID/g after 0.5 h and 24 h post-intravenous injection, respectively. Nonetheless, due to a faster clearance of radiolabeled GIP from normal muscular tissue and from the blood, the tumor/muscle (T/M) and the tumor/blood (T/B) ratios increased following post administration time (Figure 1), indicating that a notable portion of the radiopeptide was still retained in the tumor tissue. Concurrently, the

Table 3. Biodistribution of P149-Q^[125I]-Y peptide in tumor-bearing C3H/W mice (%ID/g mean and SD; n=6).*

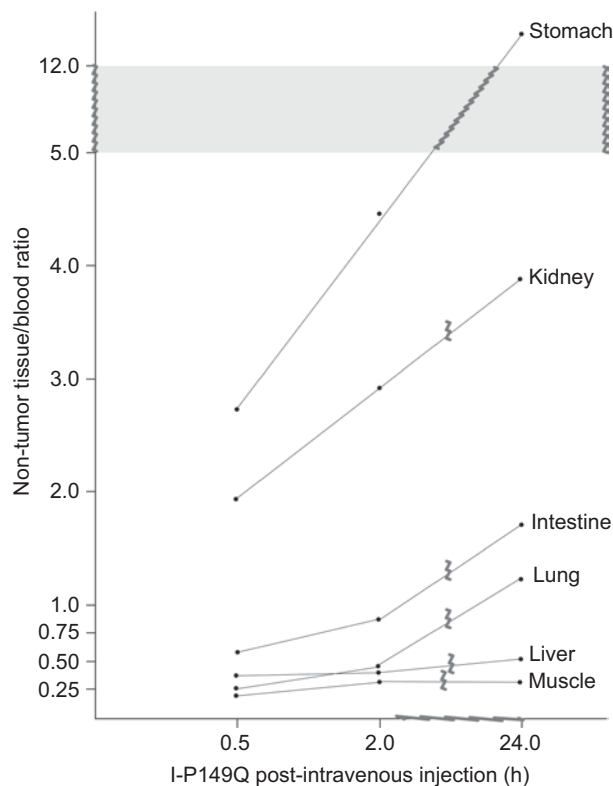
Organ/Tissue	0.5 h p.i.v.	2 h p.i.v.	24 h p.i.v.
Blood (1 mL)	6.86 ± 1.78	4.15 ± 0.37	1.65 ± 0.20
Thyroid gland	5.43 ± 1.21	6.25 ± 0.29	3.13 ± 0.65
Lung	1.78 ± 0.01	1.69 ± 0.27	2.04 ± 0.86
Liver	2.97 ± 0.62	1.68 ± 0.15	0.85 ± 0.11
Kidney	13.41 ± 1.70	12.73 ± 2.58	6.32 ± 2.49
Stomach	18.85 ± 3.44	18.60 ± 2.12	20.08 ± 4.12
Intestines	4.17 ± 0.49	3.62 ± 0.51	2.85 ± 0.19
Tumor	3.23 ± 0.41	2.83 ± 0.45	1.60 ± 0.35
Muscle	1.40 ± 0.19	1.20 ± 0.28	0.47 ± 0.02
Urine [%ID]	26.76 ± 0.98	41.10 ± 4.29	66.98 ± 7.49

*Data extracted and modified from Garnuszek et al. (2005).

**Figure 1.** Variations of *in vivo* concentration of P149-Q^[125I]Y in mouse mammary adenocarcinoma (bars) with time after administration, in relation to ratios of the tumor/muscle (solid line) and the tumor/blood (dashed line). Data extracted and re-drawn from Garnuszek et al. (2005).

nontumor-to-blood ratios in the stomach, kidney, and intestine continued to rise at 24 h post-injection indicating radionuclide uptake (Figure 2; see Discussion). Such behavior of the radioiodinated peptide *in vivo* suggests a specific mechanism of peptide binding and retention in the tumor cells, probably reflective of ligand-receptor interaction.

The two cysteines present in linear GIP-34 peptide may favor, in solution, the intrapeptide disulfide bond formation that lead to the loss of peptide activity (Muehleemann et al., 2005). For this reason, the ^{99m}Tc-labeling of the peptide and the HYNIC conjugates were performed with the use of stannous chloride for ^{99m}Tc(VII) reduction to ^{99m}Tc(IV), both in the absence and in the presence of tricaine as a co-ligand, respectively. The yields of ^{99m}Tc-labeling depend on peptide concentration, reaction time, temperature, presence or absence of co-ligand

**Figure 2.** The nontumor-to-tumor blood ratios are displayed for the biodistribution of ¹²⁵I-P149Q in various organs of C3H/W mice studied at three time intervals. Data derived and revised from Garnuszek et al. (2005).

(tricaine), and blocking of the free sulfhydryl groups with N-ethylmaleimide (EM). The HYNIC-P149-QY conjugate labeled with ^{99m}Tc in the presence of tricaine produced yields of about 95%.

In vivo experiments with the directly ^{99m}Tc-labeled P149-QY showed significant differences of biodistribution (Table 4) compared to the P149-Q^[125I]Y analogue (Table 3). ^{99m}Tc-labeled P149-QY peptide revealed a high kidney accumulation (72% ID/g), with a lower concentration in blood (2.25% ID/ml), as well as a low concentration in tumor tissue (0.66% ID/g). The introduction of HYNIC as a bifunctional chelator for ^{99m}Tc-labeling of P149-QY peptide in non-tumor mice surprisingly resulted in an increase of kidney uptake up to 156% ID/g and a decreased radionuclide accumulation in blood. Considering the biodistribution results for both direct and indirect ^{99m}Tc-labeled peptide, it seemed that ^{99m}Tc binding negatively influenced the structure of the peptide, probably due to radionuclide reaction with--SH residues (Cys8 and Cys21). After blocking of the free sulfhydryls in HYNIC-P149-QY by EM, the kidney uptake decreased to 90% ID/g, and a 50% higher excretion of the radioactivity in urine was observed (Maurin et al., 2008). This sulfhydryl blocking positively influenced the target tissue accumulation in tumor-bearing mice (Table 4).

Table 4. Biodistribution of the ^{99m}Tc -radiolabeled P149-QY peptide in normal and tumor-bearing mice (2-h post intravenous injection - p.i.v.; %ID/g).[†]

Tissue	^{99m}Tc -HYNIC-P149-QY normal Swiss mice $n=6$	^{99m}Tc -P149-QY tumor-bearing C3H/W mice $n=5$	^{99m}Tc -HYNIC-P149-QY* $n=5$
Blood (1 mL)	0.51 ± 0.18	2.25 ± 0.43	1.44 ± 0.12
Thyroid gland	0.40 ± 0.09	1.19 ± 0.44	1.33 ± 0.26
Lung	0.49 ± 0.16	1.75 ± 0.43	1.11 ± 0.08
Liver	4.66 ± 2.90	3.36 ± 1.21	4.40 ± 0.24
Kidney	156.00 ± 24.67	72.16 ± 3.35	80.76 ± 15.26
Stomach	0.40 ± 0.11	3.83 ± 1.19	1.29 ± 0.32
Intestines	0.67 ± 0.24	2.64 ± 0.54	2.55 ± 0.05
Tumor	-	0.66 ± 0.16	1.27 ± 0.26
Muscle	0.24 ± 0.08	0.37 ± 0.16	0.58 ± 0.08
Urine [%ID]	36.23 ± 10.82	39.79 ± 5.94	53.31 ± 5.40

*SH-blocked.

[†]Data extracted and modified from Maurin et al. (2008).

Figure 3 displays the comparison of the target-to-non-target ratios for the three radioactive preparations studied in tumor-bearing mice. In spite of comparable tumor/muscle (T/M) ratios observed for the three preparations, the tumor/blood (T/B) ratio is significantly higher for SH-protected ^{99m}Tc -HYNIC-P149QY (0.89 ± 0.22), especially when compared directly with ^{99m}Tc -labeled P149QY (0.28 ± 0.06). This suggests specific binding of the SH-blocked peptide in tumor tissue, not only arising from tumor vascularity and blood flow, but also due to a specific peptide accumulation based on ligand-receptor interaction.

In order to prove that GIP-34 might bind to an AFP receptor(s) in tumor tissue, an attempt was made to detect proteins that were bound to the radiopeptide in tumor tissues. Protein extracts from mouse mammary adenocarcinoma were incubated with P149-Q[^{125}I]Y in the presence of the cross-linking agent, ethylene glycol bis(succinimidyl succinate). Following Western blotting, a radioactive band with an estimated molecular weight of 30 kDa was detected (Garnuszek et al., 2005).

Cell membrane fluorescence

Both forms of GIP (linear, scrambled) were individually conjugated to the surface of EviTags (nanocrystals from Evident Technologies) quantum dots which emit a green fluorescence at 520 nm. The amount of light emitted by quantum dots remained constant regardless of the peptide's conformation and sequence (data not shown). Upon exposure to MCF-7 cells, linear GIP-EviTags localized both on the surface and in the cytoplasm of the tumor cells are shown in Figure 4A–C. Panel B displays the cell surface of MCF-7 cells incubated at 4°C with the GIP/EviTags conjugate. It was evident that the tumor cells had bound and incorporated the conjugated GIP onto the cell surface membrane. The clear definition of cell peripheries produced by the particulate fluorescence could be noted as well the less obvious nuclei barely

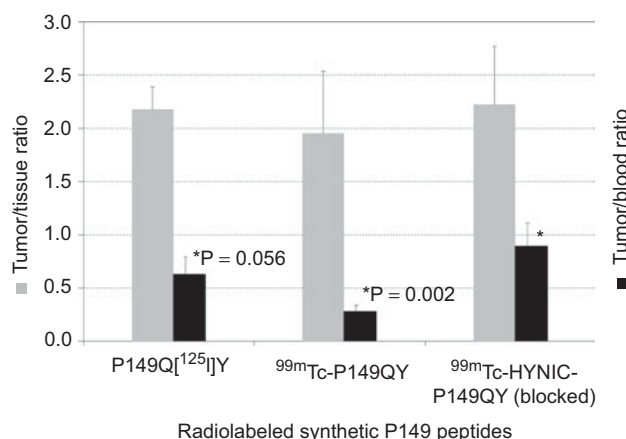


Figure 3. Comparison of the target to non-target ratios (tumor/muscle T/M, and tumor/blood T/B) for the three radioactive preparations of P149QY peptide, studied in mammary adenocarcinoma bearing C3H/W mice 2-h p.i.v. Data extracted and redrawn from Maurin et al. (2008).

made visible by a faint punctuate fluorescence. In contrast with the scrambled peptide conjugated on EviTags in Figure 4C, linear GIP clearly binds to the surface of MCF-7 cells (Figure 4B), while the former did not bind.

For isolation of a putative GIP receptor on MCF-7 cells, immediately after cell surface binding, a membrane protein (solution) extract was produced by sonication and vortexing followed by passage through a GIP-bound affinity column and purging via glycine-HCl-low pH solution (Teng et al., 2000). Eluents from the GIP column were separated according to size by SDS-PAGE analysis. All PAGE lanes produced standard bands as expected by the migration markers; however, two lanes produced a faint band which was heretofore not present in prior eluents and washings. The washings represented the supernatant from the sonication/vortexing step and the third high salt/pH wash. Following calculations in comparison to migration markers, the unknown band was calculated to have a molecular mass of 16.5 kDa.

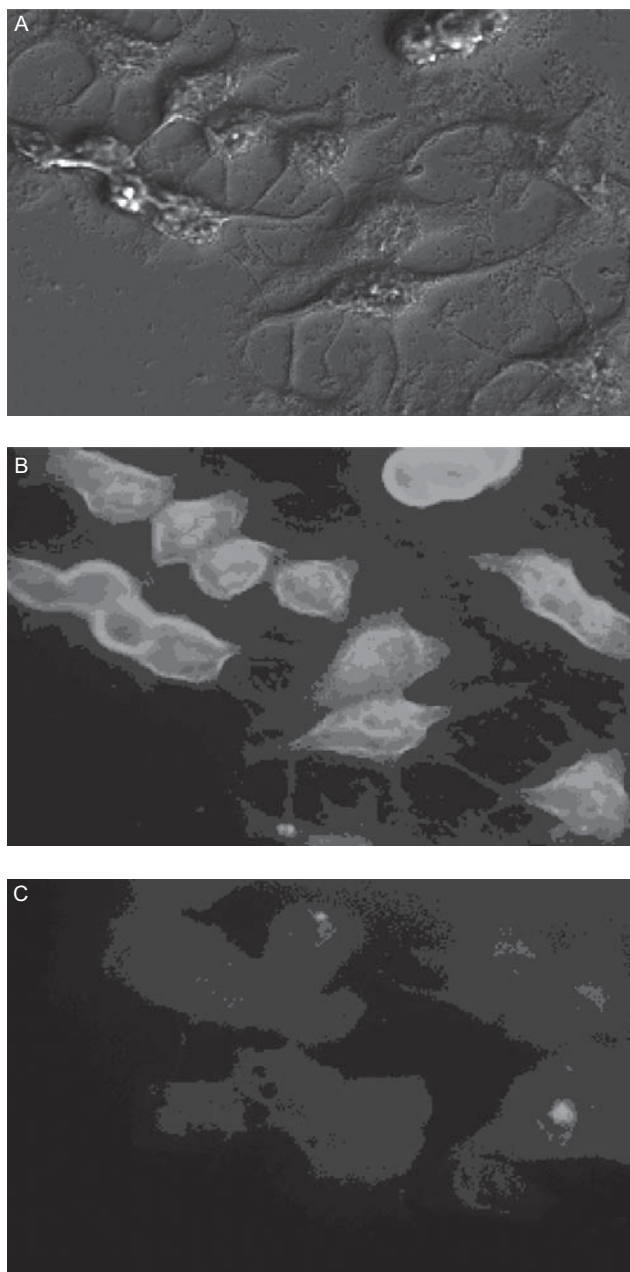


Figure 4. Microscopy of human MCF-7 cells: (A) bright field image of cells in (B). Fluorescent microscopy of MCF-7 with (B) linear GIP-34/EviTags and (C) scrambled GIP-34/EviTags. Photos obtained from Co-author's (B, D, C.) unpublished data.

Doxorubicin cytotoxicity

It has been previously reported that GIP-34 bound to the surface of MCF-7 breast adenocarcinoma cells and was then endocytosed by these cells (Mizejewski & MacColl, 2003). One of the present multicenter research groups (Severin et al., 1995) studied whether the C-terminal fragment of linear GIP-8 possessed such activity and for this purpose employed an FITC-labeled derivative of octapeptide FITC-GIP-8 (Figures 5 and 6). The binding and endocytosis of FITC-GIP-8 by human ovarian tumor

cells and normal human peripheral blood lymphocytes were monitored by flow cytometry. Peptide-to-cell binding was analyzed following a 1.0 h incubation of FITC-EMTPVNPG (GIP-8) with tumor cells at 4°C; however, endocytosis only occurred after 1 h incubation at 37°C. It was found that FITC-GIP-8 bound readily to SKOV3 ovarian cells (Figure 5A), but bound only slightly with stimulated lymphocytes (Figure 5B). The measurement of the level of endocytosis of FITC-GIP-8 thus provided evidence of high specificity of GIP-8 uptake by the ovarian tumor cells. In a similar fashion, the incubation of lymphocytes with FITC-GIP at 37°C produced little if any influence on the increase of fluorescence intensity (IFI) compared to incubation at 4°C; under the same conditions, tumor cells displayed a notable increase in the IFI. On average, the tumor cells displayed a fivefold increase and an order of magnitude increase, compared to the accumulation of FITC-GIP-8 in lymphocytes demonstrating tumor cell binding specificity.

Analysis of the endocytosis and intracellular distribution of FITC-GIP-8 with fluorescent microscopy showed that bright luminous clusters could be observed in the tumor cell cytoplasm after 1 h incubation (37°C) of cells with FITC-GIP-8 (Figure 6A). After a lapse of 24 h, the fluorescence was more intense and in juxtaposition to other clusters forming wide luminous zones in the cytoplasm, mostly in the perinuclear region of the cell (Figure 6D–F).

The GIP-8 conjugated to the antibiotic DOX was synthesized by the use of a 4(4-N-maleimidomethyl)cyclohexane-1-carboxyl hydrazide crosslinker which forms a thioester bond between the 8-mer peptide and the DOX. The accumulation and distribution of the GIP-8–DOX conjugate were then examined in SKOV3 cells using fluorescence and phase microscopy. The distinctly expressed red fluorescence of DOX in cells treated with the GIP-8–DOX conjugate (Figure 7A–H) provided evidence supported by phase microscopy that DOX was inclusive within the conjugate and was efficiently taken up by the tumor cells. As the time of incubation increased from 1 to 4 h, the fluorescence intensity increased. As shown in Figure 6, cells treated with GIP-8–DOX conjugate displayed DOX distribution predominantly in the nuclei of cells, such a phenomenon being typical for unbound (free) DOX; this indicated that DOX contained within the GIP-conjugate retained the ability to penetrate into nuclei of tumor cells to interact with the cell target DNA.

The uptake of GIP-8–DOX by several different tumor cells was detectable using flow cytometry and was observed to be a rapid process. After a 15 min incubation of cells with increasing conjugate concentrations at 37°C, a significant increase could be seen in the intensity of fluorescence of DOX within the tumor cells, and this observation was consistent with the evidence that

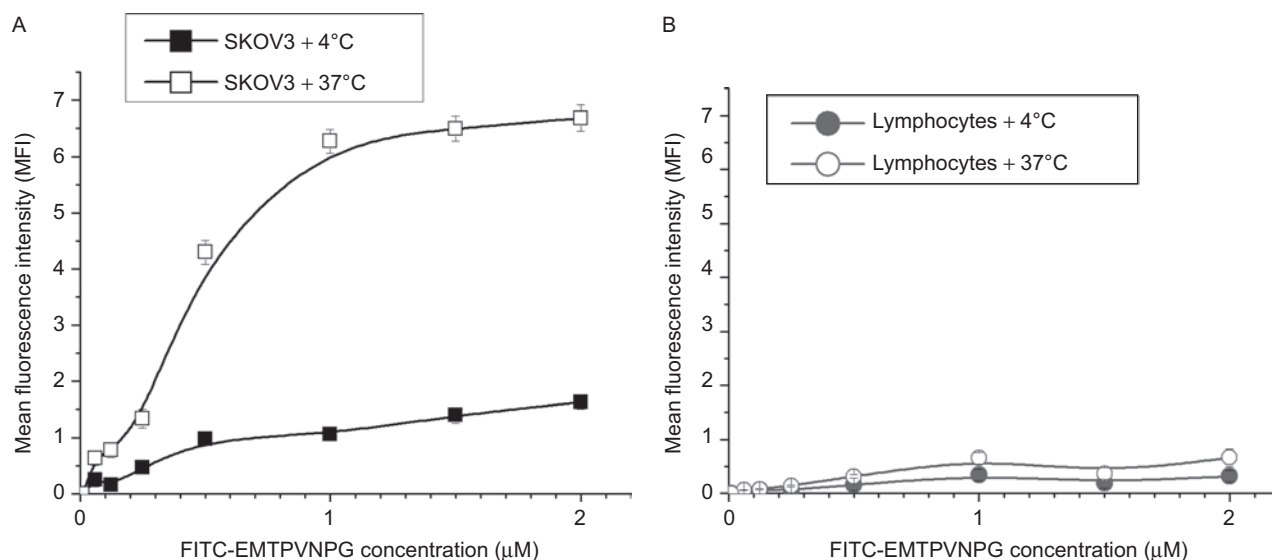


Figure 5. Binding (+4°C) and uptake (+37°C) of FITC-GIP-8(EMTPVNPG) by (A) human ovarian carcinoma SKOV3 cell line and (B) human peripheral blood lymphocytes. The Figures 5-9 were modified and redrawn from data obtained at the 30th Meeting of the Oncodevelopmental Biology & Medicine Society, Boston, MA, 2002.

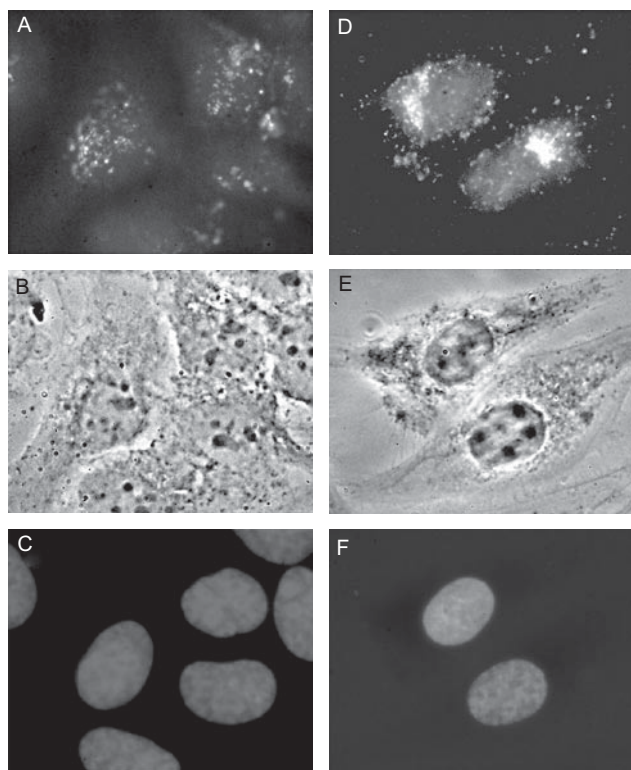


Figure 6. Intracellular localization of FITC-GIP-8(EMTPVNPG) after 1 h (A-C) and 24-h (D-F) incubation in human ovarian carcinoma cells of SKOV3 line. (A,D) Green fluorescence of FITC; (B,E) phase contrast; (C,F) blue fluorescence of the nuclei of cells, stained with Hoechst 33342. Magnification 400×. (For data source, see Figure 5 legend.)

tumor cells had engulfed, retained, and accumulated the conjugate (Figure 8). The efficiency of this process varied for the different lines of tumor cells, but in all

cases the accumulation of GIP-8-DOX exceeded the accumulation of free DOX by 2.5-fold to 15-fold. In contrast to the tumor cells, lymphocytes from peripheral blood showed accumulation of GIP-8-DOX after 15 min of incubation and did not differ from that of free DOX for the same time interval (Figure 8, bottom right panel). It is of interest that the accumulation of GIP-8-DOX in both tumor cells and lymphocytes highly correlated with the observed FITC-GIP-8 accumulation on those cells (Figure 6).

The study of cytotoxic activity of the GIP-8-DOX conjugate showed that the *in vitro* toxicity of the conjugate for SKOV3 and MCF-7 cells approximated that of the unbound (free) DOX for the same cell lines (Figure 9). Concurrently, cytotoxicity of stimulated lymphocytes due to the GIP-8-DOX was markedly lower (by one order of magnitude at the minimum) than that for unbound (free) DOX.

Discussion

GIP-34 growth effect on tumor cell lines

It has been reported that GIP-34 peptides were capable of suppressing the *in vitro* growth of a multitude of human cancer tumors in addition to breast cancers. As previously reported (Mizejewski & MacColl, 2003; Muehleemann et al., 2005), the GIP-34 segment displayed cytostatic activity in cell cultures representing eight different human tumor types and inhibiting growth in 38 of 60 different cell lines grown in 5% FBS-containing media. The effective peptide doses of tumor suppression ranged from 10^{-5} M to 10^{-7} M which encompassed glandular,

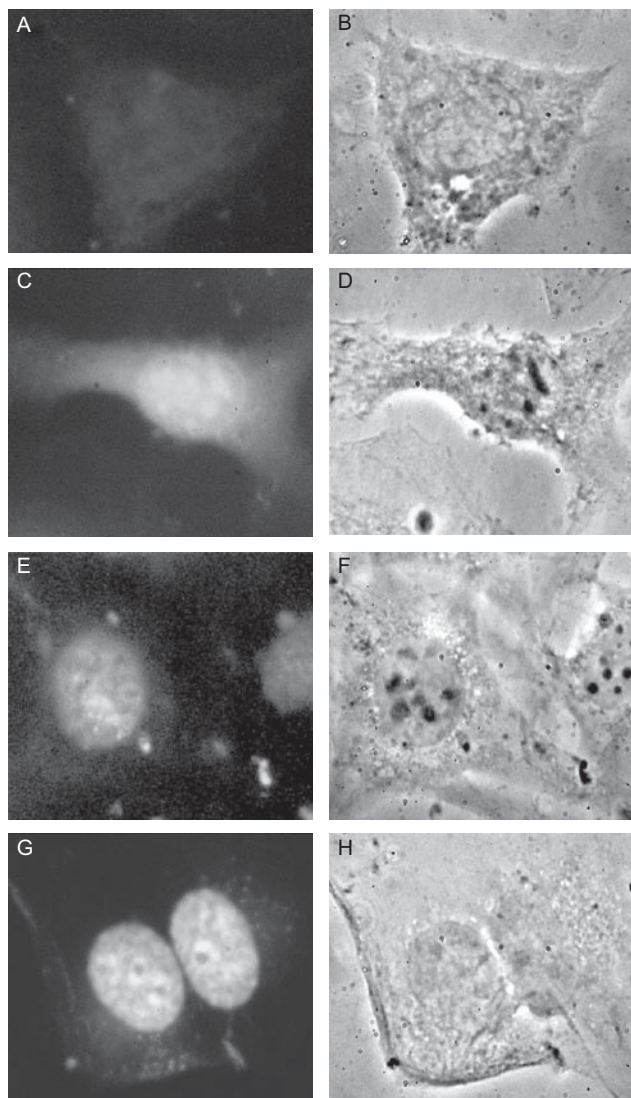


Figure 7. The distribution of GIP-8 (EMTPVNPG)-DOX conjugate in human ovarian carcinoma SKOV3 cells after (C,D) 1 h, (E,F) 4 h and (G,H) 24 h incubations. (A,B) Control cells; (A,C,E,G) fluorescence microscopy; (B,D,F,H) phase-contrast microscopy. (For data source, see Figure 5 legend.)

ductal, and epithelial carcinomas (especially breast tumors, 80%) with marginal activity against leukemias, and a lack of activity against sarcomas. In the present review, it was confirmed that the GIP suppressive activity required additional peptide doses since single dose exposure to GIP, while effective at 2 days, did not always endure for 7 days. It was further observed that GIP-34 at 2 days of treatment was as effective as tamoxifen at comparable doses, while a similar comparison to DOX (10^{-7} M) showed that the antibiotic drug surpassed GIP-34 in some of the tumor growth suppression assays. These observations suggested that DOX conjugated to GIP should be highly effective against tumors and it proved to be so (see Results section). It is further suggestive that the GIPs might even be combined (as a non- conjugate)

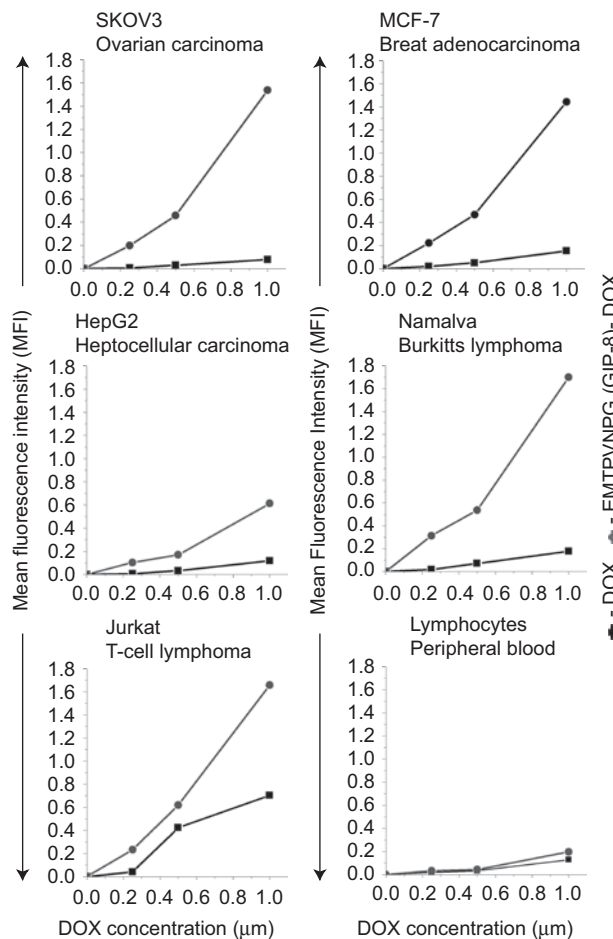


Figure 8. The uptake of doxorubicin by human tumor cells (ovarian carcinoma SKOV3, breast adenocarcinoma MCF-7, hepatocellular carcinoma HepG2, B-lymphoma Namalva, T-lymphoma Jurkat) and human peripheral blood lymphocytes after 15 min incubation with doxorubicin (DOX) and its conjugate with EMTPVNPG(GIP-8) at 37°C. MFI, mean fluorescence intensity. Closed squares, DOX; closed circles, (EMTPVNPG) GIP-8-DOX. (For data source, see Figure 5 legend.)

with DOX and/or tamoxifen doses in future experiments of therapeutic efficacy.

It was noteworthy that the GIP-34 tumor growth suppression property was also demonstrable *in vivo* using daily peptide dose injections in a 4-day hollow fiber assay (Table 1). The 4-day *in vivo* assay indicated that GIP was able to penetrate the pore size of the hollow fiber implant and was capable of suppressing growth of body cavity-implanted ovarian tumor cell lines OVCAR-3 (30%) and OVCAR-4 (42%), NCI-H226 and H460 lung cancers (33%), and breast tumors MDA-MD-231 and MDA-MD-435 (15–30%). Since GIP-34 performed best in breast and ovarian tumors, the MCF-7 breast and ovarian tumors, the MCF-7 breast tumor and the SKOV3 ovarian tumors were selected for study in various assays of the present multicenter report (see DOX toxicity later).

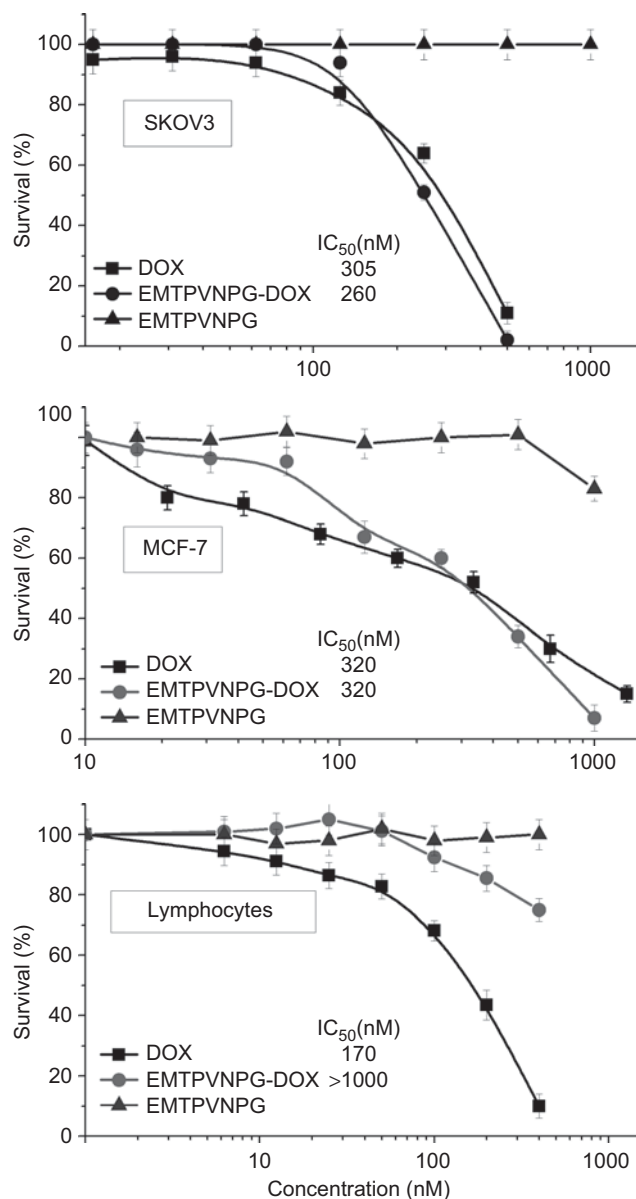


Figure 9. Viability of human ovarian carcinoma SKOV3 cells, human breast adenocarcinoma MCF-7 and stimulated lymphocytes after a 72h incubation with (EMTPVNPG)GIP-8-DOX and DOX. (For data source, see Figure 5 legend.)

Biodistribution

It has been documented that human tumor cells express cell surface proteins with binding affinity for full-length AFP (Mizejewski & MacColl, 2003). Such a receptor for AFP was first described for MCF-7 human breast cancer cells (Villacampa et al., 1984; Torres et al., 1989; Kanevsky et al., 1997). Those studies revealed the receptor's presence and showed the existence of two classes of binding sites, low (10^{-8} M) and high (10^{-10} M) affinity binding sites (Villacampa et al., 1984; Mizejewski, 1995). On the basis of these studies and others, it was observed that at least three membrane proteins with molecular masses of 18,

31, and 65 kDa were involved in the binding of AFP to breast cancer cells (Villacampa et al., 1984; Naval et al., 1985; Suzuki, Zeng, Alpert, 1992; Torres, Darracq, & Uriel, 1992a; Moro et al., 1993). The number of receptors per cell ranged from 2,000 to 300,000, including both the low- and high-affinity binding sites (Mizejewski, 1995).

In a previous study, the accumulation of radiolabeled AFP was confirmed in both mouse and rat tumors (Line et al., 1999; Mirowski et al., 2003; Maurin et al., 2008). The specific accumulation of labeled AFP in the rat mammary adenocarcinoma was significantly higher than that in rat mammary adenoma (Mirowski et al., 2003).

It was proposed that only short peptide segments of the whole AFP molecule may actually be involved in the interaction of AFP with its putative receptor (Mizejewski et al., 1996; Mizejewski, 2002). Such a concept provided the impetus for further analysis of the GIP-34 fragment synthesized as a modified 36-amino acid peptide of 90% homology to GIP-34 named the P149-QY (Garnuszek et al., 2005). The introduction of tyrosine at the C-terminal end enabled the radioiodination of the P149-Q[¹²⁵I]Y peptide which, after isolation and purification on reverse phase-HPLC, demonstrated radiochemical purity in the range of 95%, and was quite stable during storage for several days at 4°C. Biodistribution studies in tumor-bearing mice have demonstrated a higher pharmacokinetic rate of P149-Q[¹²⁵I]Y compared with the radioiodinated [¹³¹I]-AFP molecule (Mirowski et al., 2003; Garnuszek et al., 2005).

The biodistribution of radiolabeled P149 (GIP-34) deserves special mention in that the non-tumor-to-blood ratios in certain organs of the C3H mice were exceedingly high. Increased ratios above 1.0 indicated that the radionuclide/peptide conjugate had accumulated and was retained in that organ. The kidney can readily be explained by the observation that radionuclide was being eliminated via the kidney as urine levels would indicate (Garnuszek et al., 2005). However, the highly elevated ratios in the stomach were an unexpected observation. Recent publications regarding the expression of the GPR30 receptor in mouse and human tissues (Kakinuma et al., 2005; Isensee et al., 2009) may provide a possible explanation. In a study by Hamza et al., (2003) it was reported by computer modeling that a portion of GIP-34 was capable of binding to the GPR30 receptor. It was then reported (Kakinuma et al., 2005) that the expression of a GPR30 mRNA form was detected in both human normal stomach cells and in gastric cancer cells. It was subsequently reported (Isensee et al., 2009) that mice contained high expression levels of GPR30 in normal murine gastric chief cells of the stomach and in small arterial vessels of multiple tissues (intestine, lung). Thus, it can be proposed that this observation provides indirect (circumstantial) evidence of GIP binding to a GPR30 receptor-like molecule.

At present, the radionuclide used in nuclear medicine in 90% of all scans is ^{99m}Tc which is available from $^{99}\text{Mo}/^{99m}\text{Tc}$ generators. Due to the importance of ^{99m}Tc labeled peptides to radio-immunodiagnosis and because of the large notable differences between the direct and indirect methods for peptide labeling, the preferred use of ^{99m}Tc -labeled P149QY via bi-functional chelator HYNIC was highly justified (Maurin et al., 2008). Significant differences were noted in biodistribution studies between P149-Q[^{125}I]Y analogue, the directly ^{99m}Tc -labeled P149-QY, and ^{99m}Tc -labeled-HYNIC-P149-QY in spite of comparable T/M ratios observed for the three preparations (Figure 3). According to data presented by Maurin et al. (2008) it was proposed that the two cysteines present in solubilized P149 peptide favor the intrapeptide disulfide bond formation that may lead to alterations of the anti-growth activity of the peptide (Garnuszek et al., 2005). It was also observed that the presence of some ions may influence the peptide activity such as Zn(II) ion binding to the GIP-34 peptide, stabilizing its active form (Eisele et al., 2001a, 2001b; MacColl et al., 2001; Garnuszek et al., 2005); however, Co(II) ion acts in reverse, catalyzing the loss of peptide activity. Therefore, efforts were made to prevent the formation of a less active form of the peptide in the radiolabeling process, and that a new peptide analogue should be synthesized in which the two cysteine residues would form a disulfide-bridged cyclic GIP-34.

For the detection and identification of (P149-Q[^{125}I]Y)-binding proteins, methods based on chemical cross-linking between receptor and labeled ligand were utilized for the detection of GIP-34 receptor molecules in human breast cancer (Prévost et al., 1993). According to that data, (P149-Q[^{125}I]Y)-binding protein derived from the tumor extract appeared as a single band with a molecular weight of 30 kDa. From these findings, one can conclude that the interaction between AFP-peptide and its putative receptor are possible through the amino acid sequences exposed by GIP-34, and that the radioiodinated peptide in western blots identified a molecular mass of 30 kDa as a receptor for the radiopeptide. However, further studies are needed for the identification of the actual receptor responsible for binding with the radiolabeled GIP molecule.

Cell surface fluorescence

The present microscopical fluorescence analysis using nanocrystals demonstrated that conjugated GIP interacted and bound to the plasma membrane interface of individual MCF-7 tumor cells. By fluorescence tagging of GIP with EviTags quantum (nano) dots, visualization of GIP cell surface binding was achieved, while scrambled peptide controls produced little, if any, cell surface fluorescence demonstrating binding specificity. GIP is then endocytosed, packaged in vesicles (endosomes),

and passed through the trans-golgi and endoplasmic reticulum to ultimately reside in a perinuclear location (see Results section) within the cell.

In order to detect and possibly identify a putative GIP receptor, an MCF-7 tissue extract was passed through an antigen (GIP) affinity column followed by a glycine-HCl and low pH column (purging) extraction. Following PAG electrophoresis and silver staining, a discrete new protein band was observed displaying a molecular mass of 16.5 kDa. This protein had bound and was eluted from the affinity column indicating it was a GIP-binding protein from the MCF-7 cell membrane sonication preparation. Since non-specific binding proteins attached to the GIP affinity column would have been washed away, present evidence suggests that the binding entity was specific to GIP.

Doxorubicin toxicity studies

The results of the study of cytotoxicity are in good agreement with the data on accumulation and uptake of the GIP-8-DOX conjugate into tumor cells. In SKOV3 and MCF-7 tumor cells, the level of accumulation of GIP-8-DOX is rather high and the conjugate displays a high toxic activity against these cells. In lymphocytes, the level of accumulation of the conjugate is low and therefore its cytotoxic activity is also low. Thus, the obtained results provide evidence of the specificity of the GIP-DOX conjugate for uptake by tumor cells *in vitro* and demonstrates that the peptide conjugate is equally effective a cytotoxic agent as DOX alone.

These findings provide evidence of high binding and subsequent endocytosis of the octapeptide by SKOV3 ovarian tumor cells and a significantly lower (by 5–10 times) level in the case of peripheral blood lymphocytes. Thus, these data provided *in vitro* evidence of the specificity of the GIP-8 octapeptide uptake by tumor cells and permits one to consider the 8-mer peptide as a potential vehicle for targeted delivery of cytotoxic drugs to tumor cells. It remains unclear, however, which receptor on the surface of tumor cells binds the GIP-8. It has been shown earlier that GIP-34 bound to the surface of MCF-7 breast adenocarcinoma cells and was clearly endocytosed by these cells (Mizejewski & MacColl, 2003). It is unlikely that either GIP-34 or the GIP-8 segment of AFP are capable of binding with the AFP membrane receptor described by Moro et al. (1993), unless the AFP molecule is denatured or undergoes a conformational change because the GIP segment is positioned inside the AFP protein globule itself.

What is the receptor for growth inhibitory peptide?

From the studies conducted in the present multicenter report, it becomes readily apparent that GIP-34 can

bind to two or more cell surface receptors. Earlier publications based on computer modeling systems suggested plausible binding of GIP to G-coupled seven-transmembrane receptors, such as the GPR30 estrogen-binding membrane receptor (Hamza et al., 2003). The binding of GIP-34 and GIP-8 to GPR-30 might only account for the estrogen-dependent activities ascribed to GIP-34, but not its estrogen-independent actions (Mizejewski et al., 2006). It has already been reported that GIP is not exposed on native, compact circulating HAFP and only a conformational change can expose the entire GIP-34 segment in stress and shock environments (Vakharia & Mizejewski, 2000). Hence, the search for a GIP receptor must take into account that GIP represents an exposed segment of the denatured (unfolded or molten globule form) AFP molecule (Mizejewski, 2001). One must then seek a receptor family that would bind conformationally altered (transformed) AFP or free-circulating peptides. Such receptors are found in gene families of proteins related to pattern recognition binding (Pal & Wu, 2009; Srikrishna & Freeze, 2009). Both AFP and albumin have been previously reported to bind such transmembrane proteins (Torres et al., 1992a).

Acknowledgements

The writing, artwork, and library/computer research utilized in this paper were supported by internal funds from the Wadsworth Center of the New York State Department of Health, Albany, NY, USA. The authors wish to express their sincerest thanks to Ms. Tracy L. Godfrey and Ms. Jennifer L. Wright for their commitment and time expenditure in the typing and processing of the manuscript, references, and tables of this review. The authors also extend their gratitude to Ms. Rachel Moseley for her production of the skillful computer graphic artwork and illustrations presented here.

Declaration of interest

BJ Poiesz received funding from the Carol Baldwin Breast Cancer Research Fund.

References

- Bennett JA, Mesfin FB, Andersen TT, Gierthy JE, Jacobson HI. (2002). A peptide derived from alpha-fetoprotein prevents the growth of estrogen-dependent human breast cancers sensitive and resistant to tamoxifen. *Proc Natl Acad Sci USA*, 99, 2211-2215.
- Biddle W, Sarcione EJ. (1987). Specific cytoplasmic alpha-fetoprotein binding protein in MCF-7 human breast cancer cells and primary breast cancer tissue. *Breast Cancer Res Treat*, 10, 279-286.
- Butterstein G, Morrison J, Mizejewski GJ. (2003). Effect of alpha-fetoprotein and derived peptides on insulin- and estrogen-induced fetotoxicity. *Fetal Diagn Ther*, 18, 360-369.
- Butterstein GM, Mizejewski GJ. (1999). Alpha-fetoprotein inhibits frog metamorphosis: implications for protein motif conservation. *Comp Biochem Physiol, Part A Mol Integr Physiol*, 124, 39-45.
- Eisele LE, Mesfin FB, Bennett JA, Andersen TT, Jacobson HI, Vakharia DD, MacColl R, Mizejewski GJ. (2001a). Studies on analogs of a peptide derived from alpha-fetoprotein having anti-growth properties. *J Pept Res*, 57, 539-546.
- Eisele LE, Mesfin FB, Bennett JA, Andersen TT, Jacobson HI, Soldwedel H, MacColl R, Mizejewski GJ. (2001b). Studies on a growth-inhibitory peptide derived from alpha-fetoprotein and some analogs. *J Pept Res*, 57, 29-38.
- Garnuszek P, Wiercioch R, Sztajer H, Karczmarczyk U, Mirowski M. (2005). Uptake of radiolabelled modified fragment of human alpha-fetoprotein by experimental mammary adenocarcinoma: *in vitro* and *in vivo* studies. *Nucl Med Rev Cent East Eur*, 8, 6-10.
- Hamza A, Sarma MH, Sarma RH. (2003). Plausible interaction of an alpha-fetoprotein cyclopeptide with the G-protein-coupled receptor model GPR30: docking study by molecular dynamics simulated annealing. *J Biomol Struct Dyn*, 20, 751-758.
- Hollingshead MG, Alley MC, Camalier RF, Abbott BJ, Mayo JG, Malspeis L, Grever MR. (1995). *In vivo* cultivation of tumor cells in hollow fibers. *Life Sci*, 57, 131-141.
- Isensee J, Meoli L, Zazzu V, Nabzdyk C, Witt H, Soewarto D, Effertz K, Fuchs H, Gailus-Durner V, Busch D, Adler T, de Angelis MH, Irgang M, Otto C, Noppinger PR. (2009). Expression pattern of G protein-coupled receptor 30 in LacZ reporter mice. *Endocrinology*, 150, 1722-1730.
- Kakinuma N, Sato M, Yamada T, Kohu K, Nakajima M, Akiyama T, Ohwada S, Shibana Y. (2005). Cloning of novel LERGU mRNAs in GPR30 3' untranslated region and detection of 2 bp-deletion polymorphism in gastric cancer. *Cancer Sci*, 96, 191-196.
- Kanevsky VYu, Pozdnyakova LP, Aksenova OA, Severin SE, Katukov Vyu, Severin ES. (1997). Isolation and characterization of AFP-binding proteins from tumor and fetal human tissues. *Biochem Mol Biol Int*, 41, 1143-1151.
- Line BR, Feustel PJ, Festin SM, Andersen TT, Dansereau RN, Lukasiewicz RL, Zhu S, Bennett JA. (1999). Scintigraphic detection of breast cancer xenografts with Tc-99m natural and recombinant human alpha-fetoprotein. *Cancer Biother Radiopharm*, 14, 485-494.
- Lorenzo HC, Geuskens M, Macho A, Lachkar S, Verdier-Sahuque M, Pineiro A, Uriel J. (1996). Alpha-fetoprotein binding and uptake by primary cultures of human skeletal muscle. *Tumour Biol*, 17, 251-260.
- MacColl R, Eisele LE, Stack RF, Hauer C, Vakharia DD, Benno A, Kelly WC, Mizejewski GJ. (2001). Interrelationships among biological activity, disulfide bonds, secondary structure, and metal ion binding for a chemically synthesized 34-amino-acid peptide derived from alpha-fetoprotein. *Biochim Biophys Acta*, 1528, 127-134.
- Maurin M, Garnuszek P, Karczmarczyk U, Mirowski M. (2008). Studies on 99mTc-labeling of the modified fragment of human alpha-fetoprotein (P149-QY). *J Radioanal Nucl Chem*, 275, 101-107.
- Mesfin FB, Andersen TT, Jacobson HI, Zhu S, Bennett JA. (2001). Development of a synthetic cyclized peptide derived from alpha-fetoprotein that prevents the growth of human breast cancer. *J Pept Res*, 58, 246-256.
- Mesfin FB, Bennett JA, Jacobson HI, Zhu S, Andersen TT. (2000). Alpha-fetoprotein-derived antiestrogenic octapeptide. *Biochim Biophys Acta*, 1501, 33-43.
- Mirowski M, S'Witalska J, Wiercioch R, Byszewska E, Niewiadomska H, Michalska M. (2003). Uptake of radiolabelled alpha-fetoprotein by experimental mammary adenocarcinoma and adenoma: *in vivo* and *in vitro* studies. *Nucl Med Commun*, 24, 297-303.
- Mizejewski G, Smith G, Butterstein G. (2004). Review and proposed action of alpha-fetoprotein growth inhibitory peptides as estrogen and cytoskeleton-associated factors. *Cell Biol Int*, 28, 913-933.
- Mizejewski GJ. (1995). Alpha-fetoprotein binding proteins: implications for transmembrane passage and subcellular localization. *Life Sci*, 56, 1-9.

- Mizejewski GJ, Dias JA, Hauer CR, Henrikson KP, Gierthy J. (1996). Alpha-fetoprotein derived synthetic peptides: assay of an estrogen-modifying regulatory segment. *Mol Cell Endocrinol*, 118, 15-23.
- Mizejewski GJ. (2001). Alpha-fetoprotein structure and function: relevance to isoforms, epitopes, and conformational variants. *Exp Biol Med (Maywood)*, 226, 377-408.
- Mizejewski GJ. (2002). Biological role of alpha-fetoprotein in cancer: prospects for anticancer therapy. *Expert Rev Anticancer Ther*, 2, 709-735.
- Mizejewski GJ, MacColl R. (2003). Alpha-fetoprotein growth inhibitory peptides: potential leads for cancer therapeutics. *Mol Cancer Ther*, 2, 1243-1255.
- Mizejewski GJ, Muehleemann M, Dauphinee M. (2006). Update of alpha fetoprotein growth-inhibitory peptides as biotherapeutic agents for tumor growth and metastasis. *Chemotherapy*, 52, 83-90.
- Mizejewski GJ. (2007). The alpha-fetoprotein-derived growth inhibitory peptide 8-mer fragment: review of a novel anticancer agent. *Cancer Biother Radiopharm*, 22, 73-98.
- Mizejewski GJ, Butterstein G. (2006a). A Survey of functional activities of alpha-fetoprotein derived growth inhibitory peptides: review and prospects. *Curr Protein Pept Sci*, 7, 73-100.
- Moro R, Tamaoki T, Wegmann TG, Longenecker BM, Laderoute MP. (1993). Monoclonal antibodies directed against a widespread oncofetal antigen: the alpha-fetoprotein receptor. *Tumour Biol*, 14, 116-130.
- Muehleemann M, Miller KD, Dauphinee M, Mizejewski GJ. (2005). Review of Growth Inhibitory Peptide as a biotherapeutic agent for tumor growth, adhesion, and metastasis. *Cancer Metastasis Rev*, 24, 441-467.
- Naval J, Villacampa MJ, Goguel AF, Uriel J. (1985). Cell-type-specific receptors for alpha-fetoprotein in a mouse T-lymphoma cell line. *Proc Natl Acad Sci USA*, 82, 3301-3305.
- Pal S, Wu LP. (2009). Pattern recognition receptors in the fly: lessons we can learn from the *Drosophila melanogaster* immune system. *Fly (Austin)*, 3, 121-129.
- Prévost G, Provost P, Sallé V, Lanson M, Thomas F. (1993). A cross-linking assay allows the detection of receptors for the somatostatin analogue, lanreotide in human breast tumours. *Eur J Cancer*, 29A, 1589-1592.
- Severin SE, Moskaleva EYu, Shmyrev II, Posypanova GA, Belousova YuV, Sologub VK, Luzhkov YuM, Nakachian R, Andreani J, Severin ES. (1995). Alpha-fetoprotein-mediated targeting of anti-cancer drugs to tumor cells in vitro. *Biochem Mol Biol Int*, 37, 385-392.
- Severin SE. (1996). In vivo anti-tumor activity of cytotoxic drugs conjugated with human alpha fetoprotein. *Tumor Target*, 2, 299-306.
- Shields GC. (2009). Computational approaches for the design of peptides with anti-breast cancer properties. *Future Med Chem*, 1, 201-212.
- Srikrishna G, Freeze HH. (2009). Endogenous damage-associated molecular pattern molecules at the crossroads of inflammation and cancer. *Neoplasia*, 11, 615-628.
- Suzuki Y, Zeng CQ, Alpert E. (1992). Isolation and partial characterization of a specific alpha-fetoprotein receptor on human monocytes. *J Clin Invest*, 90, 1530-1536.
- Teng SE, Sproule K, Husain A, Lowe CR. (2000). Affinity chromatography on immobilized "biomimetic" ligands. Synthesis, immobilization and chromatographic assessment of an immunoglobulin G-binding ligand. *J Chromatogr B Biomed Sci Appl*, 740, 1-15.
- Torres CG, Pino AM, Sierralta WD. (2009). A cyclized peptide derived from alpha fetoprotein inhibits the proliferation of ER-positive canine mammary cancer cells. *Oncol Rep*, 21, 1397-1404.
- Torres JM, Darracq N, Uriel J. (1992a). Membrane proteins from lymphoblastoid cells showing cross-affinity for alpha-fetoprotein and albumin. Isolation and characterization. *Biochim Biophys Acta*, 1159, 60-66.
- Torres JM, Geuskens M, Uriel J. (1992b). Activated human T lymphocytes express albumin binding proteins which cross-react with alpha-fetoprotein. *Eur J Cell Biol*, 57, 222-228.
- Torres JM, Laborda J, Naval J, Darracq N, Calvo M, Mishal Z, Uriel J. (1989). Expression of alpha-fetoprotein receptors by human T-lymphocytes during blastic transformation. *Mol Immunol*, 26, 851-857.
- Uriel J, Faily-Crepin C, Villacampa MJ, Pineiro A, Geuskens M. (1984a). Incorporation of alpha-fetoprotein by the MCF-7 human breast cancer cell line. *Tumour Biol*, 5, 41-51.
- Uriel J, Villacampa MJ, Moro R, Naval J, Faily-Crepin C. (1984b). Uptake of radiolabeled alpha-fetoprotein by mouse mammary carcinomas and its usefulness in tumor scintigraphy. *Cancer Res*, 44, 5314-5319.
- Vakharia D, Mizejewski GJ. (2000). Human alpha-fetoprotein peptides bind estrogen receptor and estradiol, and suppress breast cancer. *Breast Cancer Res Treat*, 63, 41-52.
- Villacampa MJ, Moro R, Naval J, Faily-Crepin C, Lampreave F, Uriel J. (1984). Alpha-fetoprotein receptors in a human breast cancer cell line. *Biochem Biophys Res Commun*, 122, 1322-1327.